

Electromagnetic Induction from Europa's Ocean and the Deep Interior

Krishan K. Khurana and Margaret G. Kivelson

University of California, Los Angeles

Kevin P. Hand

NASA Jet Propulsion Laboratory/California Institute of Technology

Christopher T. Russell

University of California, Los Angeles

An overview of the current status of research on the electromagnetic induction sounding of Europa's ocean and deep interior is provided. After briefly reviewing the history of electromagnetic induction methods used for sounding the interiors of Earth and the Moon, we provide a basic theoretical foundation of electromagnetic wave theory for spherical bodies. Next, evidence of electromagnetic induction field in the magnetic field data from the Galileo spacecraft is presented. Results from several modeling studies and the uncertainties in the fitted parameters are presented. Sources of systematic and random noise in the observations and their effect on the induction signature are highlighted next. The implications of the derived ocean conductivities for the composition of the European ocean are discussed. Finally, we examine future prospects for multiple-frequency sounding of Europa's interior from orbiting spacecraft and observatories on the surface of Europa.

1. INTRODUCTION AND SCOPE OF THE CHAPTER

Gravity measurements from Galileo Doppler data (*Anderson et al.*, 1998) show that the moment of inertia of Europa ($=0.346 \times M_E R_E^2$, where M_E and R_E are the mass and radius of Europa) is substantially less than that expected of a uniform sphere ($0.4 \times M_E R_E^2$), implying that Europa's interior is denser than its outer layers. Detailed modeling by Anderson et al. revealed that the most plausible models of Europa's interior have an H_2O layer thickness of 80–170 km overlying a rocky mantle and a metallic core. The physical state of the H_2O layer is uncertain but speculations about a liquid ocean have been made since the realization that tidal stressing of the interior is a major heat source (*Cassen et al.*, 1979, 1980) and the age of Europa's surface is only a few tens of million years (*Shoemaker and Wolfe*, 1982; *Zahnle et al.*, 1998). Models put forward to explain chaotic terrains formed by “mobile icebergs” (*Carr et al.*, 1998), extrusion of new material along lineaments (*Greeley et al.*, 1998) and lenticulae formed by buoyant diapirs (*Pappalardo et al.*, 1998) require liquid water or a low-viscosity layer at the base of these structures. After examining most of the geological evidence available to them, *Pappalardo et al.* (1999) concluded that while a global ocean remains attractive in explaining the geological observations, its current existence remains inconclusive.

Perhaps the strongest empirical evidence for the existence of a subsurface ocean in Europa at the present time comes from the electromagnetic induction measurements provided by the magnetometer (*Khurana et al.*, 1998; *Kivel-*

son et al., 1999). The magnetic signal measured near Europa consists of several components. These are a nonvarying uniform field from Jupiter and its magnetosphere in Europa's frame (~500 nT), a cyclical component of the field of Jupiter and its magnetosphere (~250 nT at the synodic spin period of Jupiter and ~20 nT at the orbital period of Europa), Europa's induction response to the cyclical field because of its internal conductivity (~250 nT near Europa's surface), and the field from the moon/plasma interaction currents (typically 20–30 nT when Europa is outside Jupiter's current sheet and up to 200 nT when Europa is located in Jupiter's current sheet). Recent, more-advanced analyses of the induction signatures (*Hand and Chyba*, 2007; *Schilling et al.*, 2007) strongly confirm the existence of a global ocean but also point out that the physical properties of the ocean (location, thickness, conductivity) remain uncertain. In this chapter, our intention is to critically review the current state of our knowledge of Europa's induction signature and assess the effort that has gone into its modeling.

2. HISTORY OF ELECTROMAGNETIC SOUNDING OF EARTH AND THE MOON

2.1. History of Geophysical Electromagnetic Induction

Two seminal works by Arthur Schuster from the late nineteenth century laid the groundwork for electromagnetic sounding of the planetary interiors. Using Gauss' “general theory of geomagnetism,” *Schuster* (1886) demonstrated that the daily magnetic variations observed in data from sur-

face observatories on Earth could be separated into external and internal parts. In a subsequent paper (*Schuster*, 1889) using data from four widely separated magnetic observatories and the theory of electromagnetic induction in a sphere from *Lamb* (1883), *Schuster* (1889) deduced that the internal part of the observed daily magnetic variations arose from eddy currents induced in Earth's interior. The next major advance in sounding the interior of Earth was made by *Chapman* (1919), who used diurnal variation data from 21 ground observatories. Using *Schuster's* inversion technique he concluded that the conductivity of Earth is not uniform and must increase with depth. That Earth's ocean can also generate appreciable inductive fields was first realized around the same time by *Chapman and Whitehead* (1922), who showed that the ocean conductivity seriously impacts the modeling of interior from diurnal variation data. However, it was only after *Chapman and Price* (1930) used much longer wave periods obtainable from storm time disturbances (D_{st}) that it could be proved convincingly that Earth's conductivity continued to increase with depth and exceed 3.6×10^{-2} S/m beyond a depth of 250 km.

The theory of electromagnetic sounding of heterogeneous bodies was spearheaded by *Lahiri and Price* (1939), who derived expressions for spherically conducting objects whose conductivity decreased with radial distance as $\sigma = k r^{-m}$ where k and m are arbitrary constants and r is the radial distance. Using the same data as *Chapman and Price* (1930), *Lahiri and Price* (1939) showed that the conductivity jump in Earth's interior actually occurred at a depth of about 700 km and that the conductivity increase was extremely rapid with depth. Much of the modern terminology and techniques used in modern global sounding were introduced by *Banks* (1969), who showed that the dominant inducing field at periods shorter than 1 yr are generated by fluctuations in the strength of Earth's ring current and have the character of P_1^0 spherical harmonic. The response of Earth has now been characterized at periods ranging from a few hours to 11 yr (see Fig. 1).

Determining electromagnetic induction response of Earth from spacecraft data was first demonstrated by *Langel* (1975), who used data from OGO 2, 4, and 6 (see also *Didwall*, 1984). However, the technique really came of age when very accurate data from the low-Earth satellite MAGSAT became available (*Olsen*, 1999a,b). The spacecraft data have now been used to sound Earth's interior to a depth of 2700 km (*Constable and Constable*, 2004). The global, long-duration, high-precision datasets from Orsted, Orsted-2, and CHAMP spacecraft are now routinely analyzed to infer conductivity distributions in both horizontal and vertical dimensions of Earth. For some latest examples of analyses of CHAMP data we refer the reader to *Martinec and McCreadie* (2004) and *Velimsky et al.* (2006).

2.2. Induction Studies of the Moon

The Apollo Moon landings and the accompanying space program in the late 1960s and the early 1970s provided many opportunities for studying the interior of the Moon

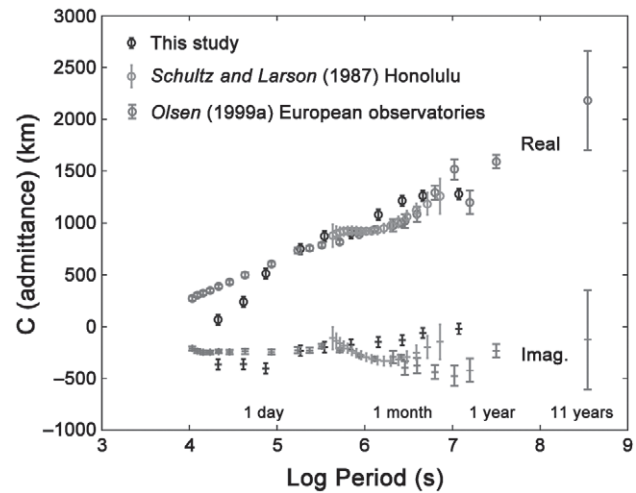


Fig. 1. See Plate 32. The response of Earth computed from data from several European surface observatories (*Olsen*, 1999a), a Hawaiian observatory (*Schultz and Larson*, 1987), and the MAGSAT spacecraft (*Constable and Constable*, 2004). The admittance function C is a rough measure of the depth to which the signal is able to penetrate in a spherical conductor and is given by $C = a[1 - (1 + 1)R]/[1(1 + 1)(1 + R)]$, where a is the radius of the Earth, R is the complex response function (ratio of the internal to external signal), and l is the degree of the harmonic. Adapted from *Constable and Constable* (2004).

from electromagnetic induction. Several orbiting spacecraft [Explorer 35 (Apoelene = 1.4 RM), Apollo 15 subsatellite (circular orbit at 100 km altitude), and Apollo 16 subsatellite (circular 100 km orbit)] made measurements of the magnetic field around the Moon. Three surface magnetometers (Apollos 12, 15, and 16) were often operated simultaneously with an orbiting spacecraft. An excellent summary of the results from the electromagnetic induction investigations is provided by *Sonett* (1982). *Schubert et al.* (1974) showed that the inductive response of the Moon to the solar wind transients is not detectable at an altitude of 100 km on the dayside because of the confinement of the induced field by the solar wind. Even though several intervals of >1-h duration from surface magnetometers were analyzed by various researchers in the early 1970s, the resulting models of lunar interior have remained nonunique (see *Sonett*, 1982; *Khan et al.*, 2006).

A technique introduced by *Dyal and Parkin* (1973) and used later by *Russell et al.* (1981) on Apollo-era data uses the response of the Moon to a step-like transient. The step-like transient in the primary field arises naturally when the Moon enters the geomagnetotail from the magnetosheath. Because the plasma flows in the magnetotail are submagnetosonic, confinement of the induced field is minimal and the data can be inverted directly for the lunar structure. Using data from 20 orbits of Lunar Prospector magnetic field data when the Moon had just entered Earth's magnetotail, *Hood et al.* (1999) estimated that the size of the lunar core is 340 ± 90 km, consistent with a value of 435 ± 15 km obtained by *Russell et al.* (1981) from the Apollo 15 and 16 data.

TABLE 1. Conductivities of common geophysical materials and their skin depths for a 10-h wave (reproduced from *Khurana et al., 2002*).

Material	Conductivity (at 0°C)		Skin depth for a 10-h wave (km)
	S/m	Reference	
Water (pure)	10^{-8}	<i>Holzappel (1969)</i>	10^6
Ocean water	2.75	<i>Montgomery (1963)</i>	60
Ice	10^{-8}	<i>Hobbs (1974)</i>	10^6
Ionosphere (E layer)	2×10^{-4}	<i>Johnson (1961)</i>	7×10^3
Granite	10^{-12} – 10^{-10}	<i>Olhoeft (1989)</i>	10^8 – 10^7
Basalt	10^{-12} – 10^{-9}	<i>Olhoeft (1989)</i>	10^8 – 3×10^6
Magnetite	10^4	<i>Olhoeft (1989)</i>	1
Hematite	10^{-2}	<i>Olhoeft (1989)</i>	10^3
Graphite	7×10^4	<i>Olhoeft (1989)</i>	0.4
Cu	5.9×10^7	<i>Olhoeft (1989)</i>	0.01
Fe	1×10^7	<i>Olhoeft (1989)</i>	0.03

3. BASIC OVERVIEW OF THE INDUCTION TECHNIQUE

According to Faraday's law of induction, a time-varying magnetic field is accompanied by a curled electric field possibly also changing with time. When a conductor is presented with such a time-varying magnetic field, eddy currents flow on its surface that try to shield the interior of the body from the electric field. The eddy currents generate a secondary induced field, which reduces the primary field inside the conductor. The electromagnetic induction technique relies on the detection and characterization of the secondary field, which contains information on the location, size, shape, and conductivity of the inducing material.

The fundamental equations governing the underlying physics of induction are

Faraday's law

$$\nabla \times \mathbf{E} = -\frac{\partial \mathbf{B}}{\partial t} \quad (1)$$

Ampere's law

$$\nabla \times \mathbf{B} = \mu_0 \mathbf{J} + \mu_0 \epsilon_0 \frac{\partial \mathbf{E}}{\partial t} \quad (2)$$

Generalized Ohm's law

$$\mathbf{J} = \sigma [\mathbf{E} + \mathbf{V} \times \mathbf{B}] \quad (3)$$

where the vectors \mathbf{E} , \mathbf{B} , \mathbf{J} , and \mathbf{V} denote electric field, magnetic field, electric current density, and flow velocity, and μ_0 is the magnetic permeability of free space, ϵ_0 is the permittivity of free space, and σ is the conductivity of the inducing material.

It is straightforward to show that these equations can be combined to yield the electrodynamic equation

$$\nabla^2 \mathbf{B} = \sigma \mu_0 \left[\frac{\partial \mathbf{B}}{\partial t} - \nabla \times (\mathbf{V} \times \mathbf{B}) \right] \quad (4)$$

where we have assumed that there are no spatial variations of conductivity in the primary conductor. In the absence of convection in the conductor, the electrodynamic equation reduces to the well-known diffusion equation

$$\nabla^2 \mathbf{B} = \sigma \mu_0 \left[\frac{\partial \mathbf{B}}{\partial t} \right] \quad (5)$$

3.1. Solutions of the Diffusion Equation in Half-Space Plane and the Concept of Skin Depth

It is instructive to examine the solution of equation (5) for a conducting half-space plane ($z > 0$) in the presence of an oscillating horizontal field ($\mathbf{B} = \mathbf{B}_0 e^{-i\omega t}$), which is given by

$$\mathbf{B} = \mathbf{B}_0 e^{-z/S} e^{-i(\omega t - z/S)} \quad (6)$$

where $S = (\omega \mu_0 \sigma / 2)^{-1/2}$ is the skin depth, a distance over which the primary signal decays by an e folding as it travels through the conductor. Equation (6) shows that the skin depth is small when the conductivity of the material is large and/or the frequency of the sounding signal is high. The equation also shows that the primary signal is phase delayed by a radian over a travel distance of one skin depth.

It can be shown that a wave with a period of 10 h (similar to that of Jupiter's spin period) has a skin depth of 30 km in a conductor that possesses a conductivity of 10 S/m (similar to that of a strongly briny solution). If the plane obstacle has a thickness larger than the skin depth of the material, the primary wave cannot significantly penetrate the obstacle and is effectively reflected back, creating the induced field that doubles the amplitude of the primary field outside the conductor. Table 1 lists skin depths for several common geophysical materials for a 10-h wave. Because of the low conductivities of pure water, ice, rocks, and an Earth-like ionosphere, the skin depths of these objects are much larger than the dimension of Europa. Therefore, these materials

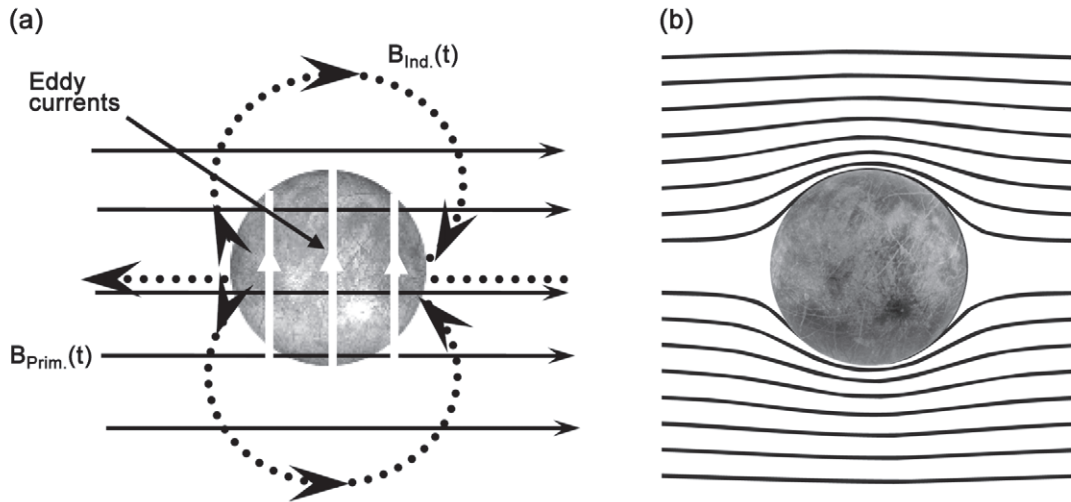


Fig. 2. (a) A time-varying primary field (black solid lines) generates eddy currents (white arrows) that flow on the surface of a conductor like Europa's ocean to prevent the primary field from penetrating the interior. The eddy currents generate an induced field (black dotted lines), which tends to reduce the primary field in the interior of the body. (b) The primary and induced fields combine such that the lines of force of the varying magnetic field avoid the conducting obstacle.

would be incapable of generating the induction response that was observed (and discussed later in section 4) by the magnetometers onboard the Galileo spacecraft. Highly conducting minerals such as magnetite or graphite and pure metals such as copper and iron have small skin depths but are unlikely to be localized in large amounts in the icy or liquid layers of Europa to produce the observed induction signal. However, a salty subsurface ocean with a conductivity similar to that of Earth's ocean and a thickness of tens of kilometers would be able to produce a significant induction response.

3.2. Diffusion Equation Solutions for Spherical Bodies

For a spherical conductor, an examination of the field at its boundary shows that when the primary field is uniform (i.e., of degree $l = 1$ in external spherical harmonics), the induced field outside the conductor would also be of degree 1 in the internal spherical harmonics, i.e., it would be dipolar in nature (see *Parkinson, 1983*). The secondary field would have the same frequency as the primary field but can be phase delayed. The primary and secondary fields sum together to form a total field, which avoids the spherical conductor (see Fig. 2). At Europa's location, the primary oscillating field is provided by Jupiter because its dipole axis is tilted by $\sim 10^\circ$ with respect to its rotational axis. In each jovian rotation, the magnetic equator of Jupiter moves over Europa twice, causing changes in the direction and strength of the field sampled by Europa. In a coordinate system called $E\phi\Omega$ centered at Europa, in which the x axis points in the direction of plasma flow (Jupiter's azimuthal direction, ϕ), the y axis points toward Jupiter and the z axis points along the rotation axis of Jupiter (Ω), B_z remains

relatively constant, whereas both B_x and B_y vary cyclically at the synodic rotation period of Jupiter (11.1 h). The amplitude of the oscillating field is ~ 200 nT at this frequency. In addition, because of the slight eccentricity ($\epsilon = 0.009$) of Europa's orbit and local time variations in the jovian magnetospheric field, Europa also experiences variations in the B_z component at the orbital period of Europa (85.2 h). The amplitude of the primary signal at this frequency is estimated to be between 12 and 20 nT, depending on the field and plasma conditions in the magnetosphere.

Following *Zimmer et al. (2000)* and *Khurana et al. (2002)*, a three-shell model of Europa (see Fig. 3) can be used to understand Europa's response to the sinusoidal uniform field of Jupiter and its magnetosphere. In this model, the outermost shell of Europa consists of solid ice, has an outer radius r_m equal to that of Europa, and possesses zero conductivity. The middle shell consisting of Europa's ocean is assumed to have an outer radius r_o and conductivity σ . The innermost shell consisting of silicates is again assumed to have negligible conductivity and a radius r_1 . As discussed above, because the primary field is uniform (degree 1, external harmonics) and the assumed conductivity distribution has spherical symmetry, the induced field observed outside the conductor ($r > r_o$) would be dipolar (degree 1, internal harmonics) (*Parkinson, 1983*). Thus

$$\mathbf{B}_{\text{sec}} = \frac{\mu_0}{4\pi} [3(\mathbf{r} \cdot \mathbf{M})\mathbf{r} - r^2\mathbf{M}]/r^5 \quad (7)$$

The dipole moment of the induced field is opposite in direction to the primary field and is phase delayed

$$\mathbf{M} = -\frac{4\pi}{\mu_0} A e^{i\phi} \mathbf{B}_{\text{prim}} r_m^3 / 2 \quad (8)$$

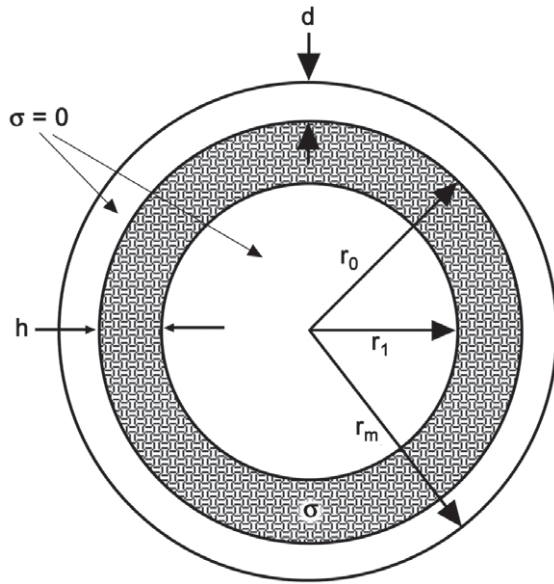


Fig. 3. Three-shell conductivity model of Europa.

Thus

$$\mathbf{B}_{\text{sec}} = -Ae^{-i(\omega t - \phi)}\mathbf{B}_{\text{prim}}[3(\mathbf{r} \cdot \mathbf{e}_0)\mathbf{r} - r^2\mathbf{e}_0]r_m^3/(2r^5) \quad (9)$$

The parameters A (relative amplitude, also known as response function) and ϕ (phase lag) are given by the following complex equations (Parkinson, 1983)

$$Ae^{i\phi} = \frac{r_0^3 RJ_{5/2}(r_0k) - J_{-5/2}(r_0k)}{r_m^3 RJ_{1/2}(r_0k) - J_{-1/2}(r_0k)} \quad (10)$$

$$R = \frac{r_1kJ_{-5/2}(r_1k)}{3J_{3/2}(r_1k) - r_1kJ_{1/2}(r_1k)} \quad (11)$$

where $k = (1 - i)\sqrt{\mu_0\sigma\omega/2}$ is the (complex) wave vector and J_m is the Bessel function of first kind and order m.

The amplitude response of Europa to the two main frequencies is shown in contour plots of Fig. 4. For plots of phase delay, we refer the reader to Zimmer et al. (2000). It was assumed that the wave amplitude of the inducing field at the synodic rotation period of Europa is 250 nT and the wave amplitude at the orbital period is 14 nT. As expected, for higher ocean conductivities and thicker ocean shells, the induction response is higher. For oceans whose height integrated conductance (conductivity \times thickness) exceeds 4×10^4 S, the amplitude response is close to unity and the phase delay is insignificant ($<10^\circ$) at the spin frequency of Jupiter. Because of noise in the data from plasma effects, the induction signal is not accurate enough to perform inversion of data using phase delay as information.

It can be seen in Fig. 4 that if the ocean thickness is less than 20 km or the ocean conductivity is less than 0.2 S/m,

the response curves of the two frequencies are essentially parallel to each other. In this regime, only the product of the ocean conductivity and its thickness can be determined uniquely. However, when the ocean thickness exceeds 100 km and the conductivity is greater than 0.2 S/m, the response curves of two frequencies intersect each other. For $\sigma > 0.2$ S/m and $h > 100$ km it is often possible to uniquely determine the ocean thickness and its conductivity if the response factors of 11.1-h and 85.2-h period waves are known. However, even in this parameter range, often only lower limits can be placed on the conductivity and thickness.

4. GALILEO OBSERVATIONS, THEIR INTERPRETATION, AND UNCERTAINTIES

4.1. Field and Plasma Conditions at Europa's Orbit

Europa is located at the outer edge of Io's plasma torus (radial distance $9.4 R_J$) where the plasma sheet is thin (half thickness $\sim 2 R_J$) and the plasma is mostly derived from Io (Bagenal and Sullivan, 1981; Belcher, 1983). Because Jupiter's dipole axis is tilted by 9.6° from its rotational axis,

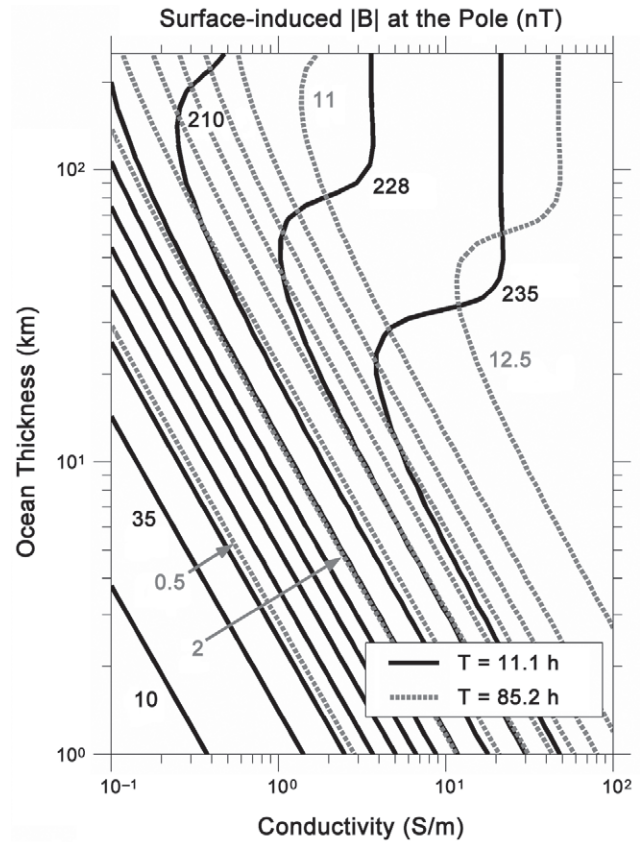


Fig. 4. The dipolar surface induction field created by the interaction of Europa with Jupiter's varying field at the two principal frequencies ($T = 11.1$ h and $T = 85.2$ h) for a range of conductivities and ocean shell thicknesses. Adapted from Khurana et al. (2002).

the plasma sheet located in the dipole equator near Europa moves up and down relative to Europa at the synodic rotation period of Jupiter (11.1 h). Therefore, the plasma density sampled by Europa changes by almost an order of magnitude at Europa over a jovian rotation with the maximum density observed near the center of the plasma sheet ($n_e \sim 50 \text{ cm}^{-3}$). The magnetic field strength varies from 400 nT (at the center of the plasma sheet) to ~ 500 nT (at the edge of the plasma sheet). In the $E\phi\Omega$ coordinate system introduced above, the dominant component of the background magnetic field is directed in the $-z$ direction and remains fairly constant over the synodic rotation period of Jupiter (11.1 h). However, the x and y components vary with amplitudes of ~ 60 nT and ~ 200 nT, respectively, over this period. Figure 5 shows a hodogram of the oscillating field in the x - y plane calculated from the magnetospheric field model of *Khurana* (1997). Also marked on the figure are the instantaneous field conditions for five close flybys of Galileo during which evidence of electromagnetic induction from Europa was observed.

As mentioned earlier, Europa also experiences a nearly harmonic perturbation in the z component of the magnetic field at its orbital period (85.2 h) with an amplitude of 12–20 nT. The main cause of this perturbation field is the day/night asymmetry of Jupiter's magnetospheric field (see *Khurana*, 2001), but the slight eccentricity of Europa's orbit also contributes.

4.2. Interaction of Europa with the Jovian Plasma

As the corotational velocity of the jovian plasma is much larger than the Keplerian velocity of Europa, the plasma continually overtakes Europa in its orbit. Because of its

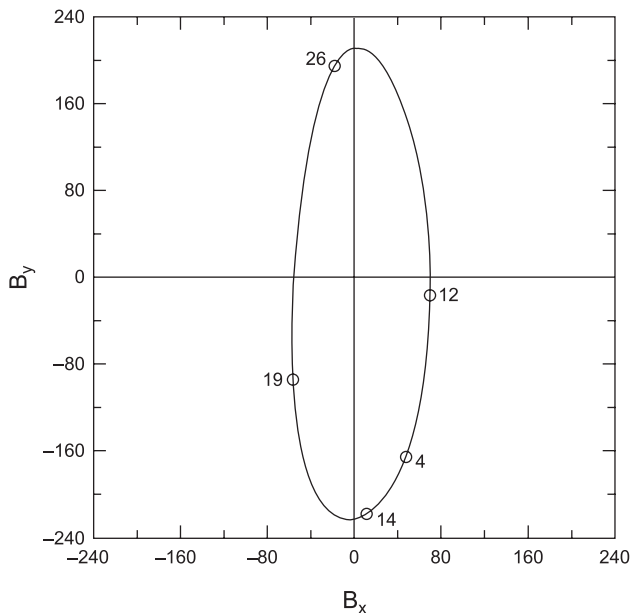


Fig. 5. The time-varying field experienced by Europa in a synodic rotation period of Jupiter.

conducting ionosphere, Europa presents itself as an obstacle to the flowing conducting plasma. The conducting exterior of the satellite extracts some momentum from the flow, slowing it upstream, but a large part of the plasma is diverted around it. Additional slowing of plasma occurs on account of plasma pickup from electron impact ionization, photoionization, and charge exchange between the plasma and the neutral atmosphere (because these processes extract momentum from the background flow). *Goertz* (1980) and *Neubauer* (1998) have shown that plasma pickup processes can be correctly treated by including a plasma pickup conductivity term in the momentum equation.

Currents flow in the conducting regions of Europa (ionosphere and the plasma pickup region) that try to accelerate Europa's ionosphere and the newly picked-up plasma toward corotation. The currents are eventually closed in Jupiter's ionosphere through a pair of Alfvénic disturbances (called the Alfvén wings) that couple the satellite's environment to the northern and southern ionospheres of Jupiter (see Fig. 6 in the chapter by *Kivelson et al.*). The slowing down of plasma in the upstream region enhances the strength of the frozen-in flux, whereas in the wake region the field strength diminishes because plasma is reaccelerated to corotation. *Neubauer* (1980) showed that the total interaction current flowing in the system is limited by the Alfvén conductance $\Sigma_A = 1/(\mu_0 V_A)$ of plasma to $I = 2\Phi\Sigma_A = 4V_0 R_m (\rho/\mu_0)^{1/2}$; here V_A is the Alfvén velocity of the upstream plasma, Φ is the electric potential imposed by the flow (V_0) across the moon, and R_m is the effective size of the moon. *Neubauer* (1999) has shown that the effective size of the obstacle (and therefore the size of the Alfvén wing) is reduced by an electromagnetic induction response from the interior of a moon because induction impedes the closure of field-aligned currents through the ionosphere of the moon by reducing the number of field lines intersecting the moon. *Volwerk et al.* (2007) show that the electromagnetic induction indeed shrinks a cross-section of the Alfvén wing of Europa by as much as 10%.

The strength of the moon/plasma interaction depends strongly on the location of Europa with respect to Jupiter's magnetic equator because both the density of Europa's tenuous sputtered atmosphere and the Alfvén conductance depend strongly on the density of upstream plasma. In order to minimize the effects of plasma interaction currents on the observed magnetic induction signature, flyby times of Europa are favored when it is located outside Jupiter's plasma sheet. In Fig. 5, these times correspond to the situations when the y component of the background field is either strongly positive (Europa located in the southern lobe of Jupiter's magnetosphere) or strongly negative (Europa located in the northern lobe). Conversely, when Europa is located near the center of the plasma sheet ($B_y \approx 0$), the expected dipole moment is weak and the noise from the plasma interaction fields is at its maximum.

The field generated by the moon/plasma interaction currents is a major source of systematic error for the induction signal. The contribution of the moon/plasma interac-

tion currents to the measured field can be assessed from magnetohydrodynamic (MHD) simulations of the interaction. The chapter by Kivelson et al. provides an excellent review of the moon/plasma interaction effects and the available MHD models of this interaction. As discussed by Kivelson et al., the only model that treats the MHD interaction of Europa and the induction from the ocean self-consistently is that of Schilling et al. (2007), whose self-consistent model shows that the strength of the interaction field is on the order of 20–30 nT even when Europa is located outside the current sheet. By using prevailing field and plasma conditions for each of the flybys of Galileo in their MHD model, Schilling et al. (2007) have greatly improved upon the determination of the Europa induction field, enabling them to place better constraints on the conductivity and the thickness of Europa's ocean. We return to the discussion of results from this model below.

Another source of noise in the observations is perturbations from the MHD waves, which transmit energy between different regions of the magnetospheres and couple them. Khurana and Kivelson (1989) have shown that the amplitudes of the compressional and transverse waves peak at the center of Jupiter's plasma sheet. The peak amplitude of MHD waves is not very large (<5 nT) near Europa because of the low- β plasma conditions at the orbital location of Europa. As the waves have high frequencies (wave periods of minutes to tens of minutes), they may not be able to penetrate the icy crust, reducing their usefulness for electromagnetic sounding of the ocean.

Finally, ion cyclotron waves generated by the pickup of plasma in the vicinity of Europa create additional noise in the observed field. Volwerk et al. (2001) show that the intensity of these waves can approach 20 nT in the wake region of Europa. Their wave periods are between 3 s and 10 s and some of the most intense waves occur with a period of ~ 5 s, corresponding to that of O_2^+ , a major constituent of Europa's sputtered atmosphere. The effect of ion cyclotron waves can be reduced on the observations by a judicious averaging and/or filtering of the data.

4.3. Galileo Observations of Electromagnetic Induction

Galileo encountered Europa 11 times, during which its closest approach altitude was less than $2 R_E$. Three of the magnetic field recordings (E6, E16, and E18) were lost because of instrument or spacecraft malfunctions. Out of the remaining eight passes, only five passes (E4, E12, E14, E19, and E26) had Europa altitudes of 2000 km or less, required for an adequate signal-to-noise ratio to decipher the induction field. The magnetic field observations from the E4 and E14 passes formed the basis for the discovery of induction response from Europa (Khurana et al., 1998; Kivelson et al., 1999) and are reproduced in Fig. 6. An examination of these figures shows that the signature is both global and dipolar in character as expected of an induction field from an ocean. It must be mentioned here that Neubauer et al. (1998) and

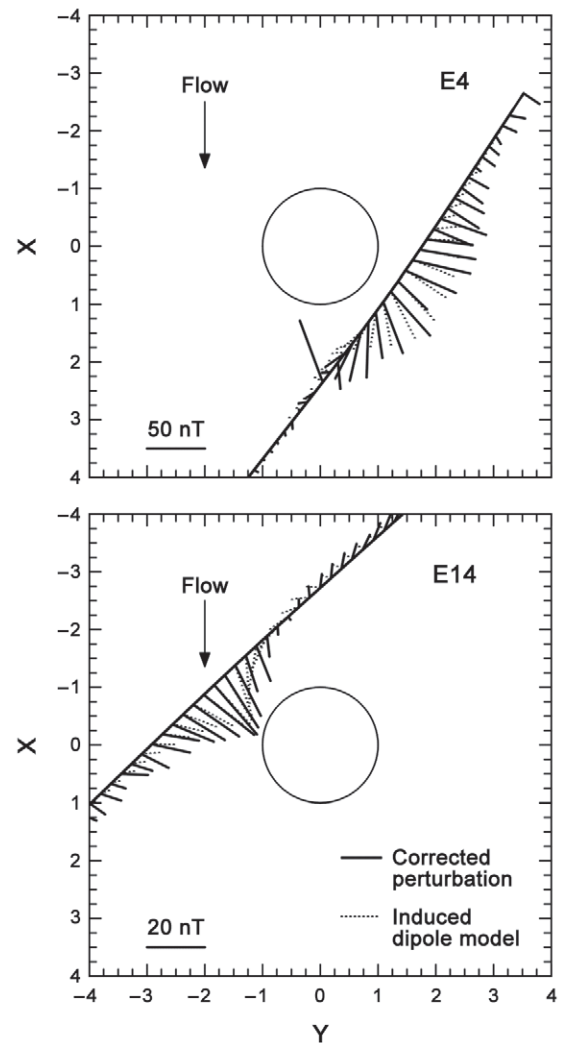


Fig. 6. The perturbation field near Europa measured by Galileo during the E4 and E14 flybys (solid vectors) and that expected from induction from a global perfect conductor (dashed vectors). Adapted from Khurana et al. (2002).

K. Kuromoto et al. (1998, unpublished manuscript made available to the magnetometer team) also independently postulated that the source of magnetic perturbations observed near Europa in the Galileo data was electromagnetic induction from an internal source.

The primary field during the E4 and E14 encounters was directed in the negative y direction (see Fig. 5). According to equations (7) and (8), the dipole moment of the secondary field would be directed in the positive y direction for both of these flybys. In order to exclude the possibility that the source of the observed dipole moment was an intrinsic internal dipole tilted toward the y axis, the Galileo magnetometer team designed a flyby (E26) during which the inducing field was directed mainly in the positive y direction (see Fig. 5). The observations from that flyby confirmed that the induced dipole moment had indeed flipped in direction and was directed in the negative direction, confirming that

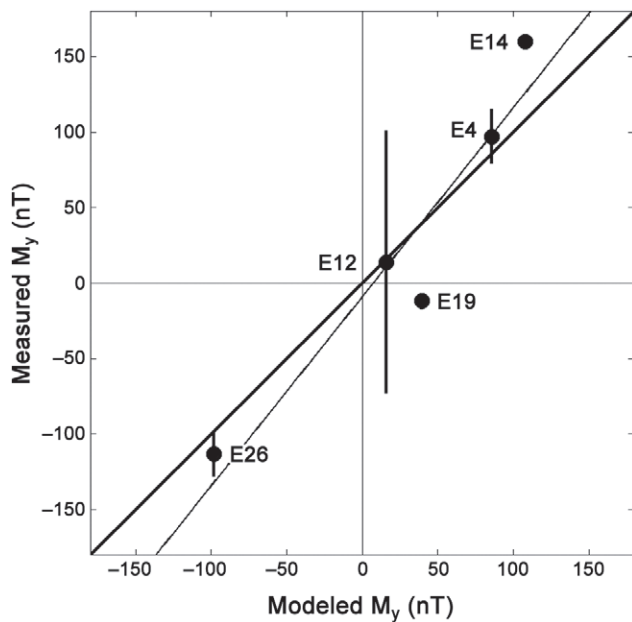


Fig. 7. The y component of the induced dipole moment measured during the five flybys of Galileo (y axis) plotted against the modeled dipole moment. Adapted from *Kivelson et al. (2000)*.

the induced field was indeed a response to the changing field of Jupiter (*Kivelson et al., 2000*). Figure 7 shows the y components of the observed dipole moments from five Galileo flybys plotted against those expected from a perfect spherical conductor with a radius equal to that of Europa. The agreement between the observations and the simple model over a large range of the excitation field provides a compelling evidence of a global conducting layer in Europa. As discussed in section 3, a consideration of various geological materials to explain the internal conductivity naturally leads to the conclusion that a present-day ocean exists in Europa.

4.4. Limits on the Induction Response

Further modeling of Europa data has been performed by *Zimmer et al. (2000)*, *Schilling et al. (2004)*, and *Schilling et al. (2007)* to place better limits on the induction response from Europa's ocean. The effect of plasma interaction on the field was modeled by *Zimmer et al. (2000)* for the E4 and E14 flybys by using a simple plasma correction model originally suggested by *Khurana et al. (1998)*. Their plasma correction model assumes that near the equatorial plane of Europa, the moon/plasma interaction currents produce mainly a compressional signal and no bending of the field is involved. In order to further simplify the data fitting procedure, *Zimmer et al. (2000)* also assumed that the phase delay of the induced signal is zero. Figure 8 shows results from their study for the E14 flyby where models with induction response factor A (ratio of inducing field to induction response) from 0.4 to 1.6 are displayed. It can be seen that models for which $A < 0.7$ or $A > 1.0$, the fits to data

are perceptibly poor. *Zimmer et al.* therefore concluded that the response factor lies between 0.7 and 1.0. The lower limit on the induction factor requires that the conductivity of the ocean must exceed 58 mS/m for an infinitely thick ocean. *Anderson et al. (1998)* place an upper limit of 170 km for the H_2O layer on Europa, which would raise the minimum conductivity of the ocean to 72 mS/m. If the ice and water layers together were only 100 km thick, the minimum conductivity required jumps to 116 mS/m.

Schilling et al. (2004) modeled the Galileo observations from four flybys (E4, E14, E19, and E26) using a Biot-Savart model of the Alfvénic current system and several different models of the permanent and induced internal field. They found that the internal field models that fit the data best and required the least number of fit parameters favored induction from an internal conducting source. In addition, the permanent internal dipole term was found to be quite small (< 25 nT at the surface of Europa). The model favored by *Schilling et al. (2004)* yields an induction factor of 0.97 from the internal ocean, suggesting that the ocean water is extremely conducting.

Schilling et al. (2007) have developed a fully self-consistent three-dimensional simulation of temporal interaction of Europa with Jupiter's magnetosphere. Their model simultaneously describes the plasma interaction of Europa's atmosphere with Jupiter's magnetosphere and the electromagnetic induction response of the subsurface ocean to the varying field of Jupiter. The mutual feedbacks — where the plasma interaction currents affect the amplitude of induction, and the induction field affects the plasma interaction by reducing the size of the Alfvén wings — are included. Figure 9 reproduced from their work shows observed and modeled fields for the E14 and E26 flybys. The vastly improved fits to the data allow *Schilling et al.* to place better-constrained limits on the ocean conductivity and thickness. They find that the conductivity of Europa's ocean would have to be 500 mS/m or larger to explain the observations made by Galileo. In addition, they favor an ocean thickness of < 100 km. However, ocean thicknesses greater than 100 km cannot be ruled out because for sufficiently large conductivities, the induction response becomes insensitive to the location of the lower boundary of the ocean. This can be verified by an examination of top right portion of Fig. 4, which shows that the induction response saturates completely for ocean thickness of > 100 km (i.e., the amplitude response curves become vertical for large conductivity values). The height-integrated conductivity of the ocean (conductivity \times ocean thickness) was found to be $\geq 5 \times 10^4$ S by *Schilling et al. (2007)*.

Because of the limited durations of the Galileo flybys of Europa, it has not yet been possible to decompose the observed induction signal into various primary frequencies and various internal and external spherical harmonics. The induction response has been modeled under the assumption that Europa experiences only a single primary frequency (at the synodic rotation period of Jupiter) whose amplitude is computed from a magnetospheric model of Jupiter. As

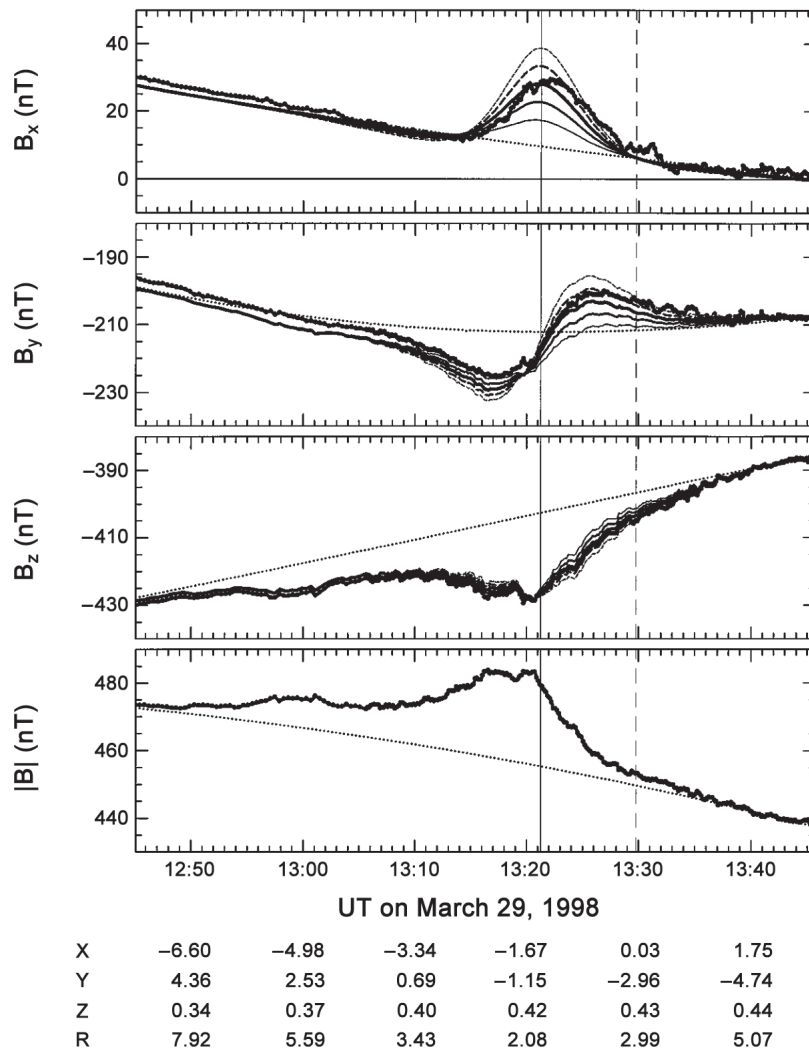


Fig. 8. Data from the E14 flyby (thick dots) and model fits for $A = 0$ (thin dotted lines), 0.4 (thin solid line), 0.7 (intermediate thickness solid line), 1 (thick solid line), 1.3 (thin dashed line), and 1.6 (thick dashed line). Adapted from *Zimmer et al. (2000)*.

discussed above, Europa does experiences a nearly harmonic perturbation in the z component of the magnetic field at its orbital period (85.2 h) with an amplitude of 12–20 nT. However, reliable estimates of the inducing field at this frequency are not yet available. In addition, as discussed in the next section, the induction caused by the ionospheric and surrounding plasma also contributes to the observed induced magnetic field and its effect should be carefully removed from the data.

5. EFFECT OF EUROPA/PLASMA INTERACTION ON THE INDUCTION SIGNATURE

In addition to generating “noise” in the magnetic data through its interaction with the jovian plasma, Europa’s interacting ionosphere also contributes to the electromagnetic induction signature through its conductivity. As dis-

cussed in the chapter by McGrath et al., the thin ionosphere of Europa has a scale height of ~200 km below an elevation of 300 km with a peak electron density in the range of 10^3 – 10^4 cm⁻³ near the surface (*Kliore et al., 1997, 2001*). As discussed by *Zimmer et al. (2000)*, in any ionosphere, the Pedersen conductivity is maximized at a location where the electron cyclotron frequency and the electron-neutral collision frequencies are equal and the maximum value is given by $\sigma_p < n_e e / 2B$ where n_e is the electron density and e is the electron charge. Using the maximum density of Europa’s ionospheric plasma as an input, they find that the Pedersen conductivity is everywhere less than 2.2 mS/m below an altitude of 300 km and less than 0.5 mS/m above 300 km. These are theoretical upper bounds on Pedersen conductivity in Europa’s ionosphere; the actual values are expected to be many times lower. For example, a self-consistent three-dimensional neutral and plasma model of Europa’s atmosphere by *Saur et al. (1998)* yields height-

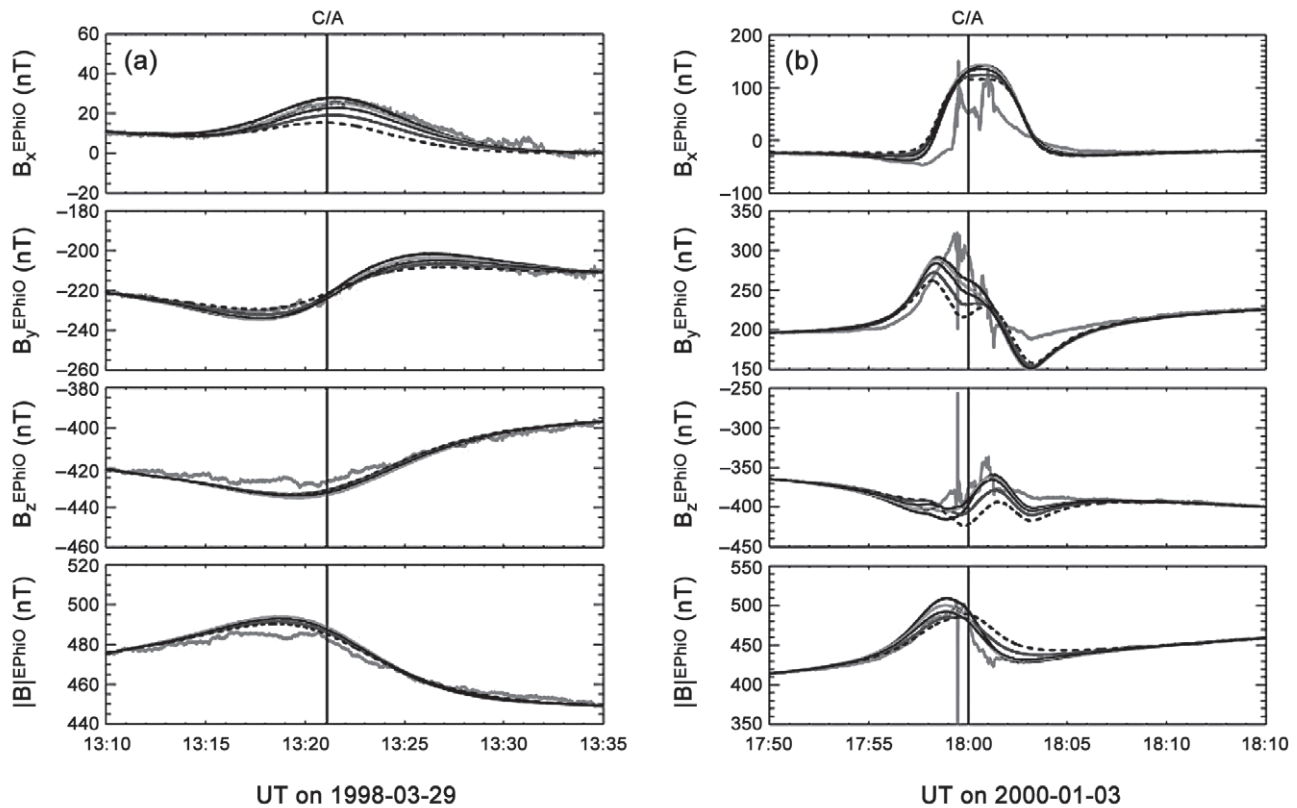


Fig. 9. See Plate 33. Observed and modeled magnetic field for the (a) E14 and (b) E26 flybys in the EfW coordinate system. Shown in the four panels are the three components and the magnitude of the observed field (red curves), model field with no induction (dashed blue), ocean conductivity 100 mS/m (blue), 250 mS/m (brown), 500 S/m (green), and 5 S/m (black). The ice thickness is 25 km and the ocean thickness is 100 km in these simulations. Adapted from Schilling *et al.* (2007).

integrated ionospheric conductivities in the range of 10–60 S, which are more than an order of magnitude lower than the theoretical upper bounds. This height-integrated conductivity should be compared with that of Europa’s ocean ($\sim 5 \times 10^4$ S) derived by Schilling *et al.* (2007). Thus, the contribution of the ionosphere to the observed electromagnetic induction signature is expected to be extremely modest.

Schilling *et al.* (2007) have computed the time-stationary and time-varying harmonic dipole and quadrupole coefficients of the plasma-induced magnetic fields over Jupiter’s synodic period from their three-dimensional simulations. They assumed an ocean thickness of 100 km and an ice crust thickness of 25 km for one of their simulations. The simulation shows that the quadrupole terms dominate over the dipole terms for both time-stationary and time-varying components at least by a factor of 2 (see Fig. 10). The dominant time-stationary term is G_2^1 with an amplitude of -29 nT. For a perfectly symmetric conductor, no plasma-induced dipole component would be expected. However, the Alfvén wings associated with the plasma interaction break the symmetry and helps generate a dipolar response (~ 12 nT) at zero frequency. The dominant time-varying quadrupolar term is g_2^1 , which has an amplitude of 14 nT and a frequency twice that of the synodic rotation period of Jupiter. The power in the induced octupole is much smaller than that of the dipole and quadrupole terms. The strongest time-varying dipolar perturbation occurs when Europa is immersed

in the plasma sheet of Jupiter ($\Omega t = 270^\circ$) and is equal to ~ 12 nT. The amplitudes of the plasma-induced Gauss coefficients are much smaller than those generated in response to the varying magnetic field of Jupiter (~ 250 nT). However, careful strategies would be required to remove the effects of plasma-generated induction fields from the observations.

6. IMPLICATION OF IMPLIED OCEAN CONDUCTIVITIES FOR THE COMPOSITION OF THE OCEAN

Most of the theoretical and experimental studies of ocean composition suggest that if the salts in Europa’s ocean arose from leaching or aqueous alteration of rocks with composition akin to those of carbonaceous chondrites, the dominant salts would be hydrated sulfates of Mg and Na (Kargel *et al.*, 2000; Zolotov and Shock, 2001; Fanale *et al.*, 2001). This conclusion is supported by Galileo’s Near Infrared Mapping Spectrometer (NIMS) surface spectral analysis of relatively young terrains (McCord *et al.*, 1998, 1999, 2001, 2002), which exhibit water-absorption bands distorted by the presence of hydrated sulfate-bearing minerals. McKinnon and Zolensky (2003) caution against a sulfate-rich model, arguing that the original chondritic material may have been much more reducing and sulfidic than assumed in most models. They place an upper limit of MgSO_4 concentrations at $100 \text{ g MgSO}_4 \text{ kg}^{-1} \text{ H}_2\text{O}$ but suggest scenarios where the

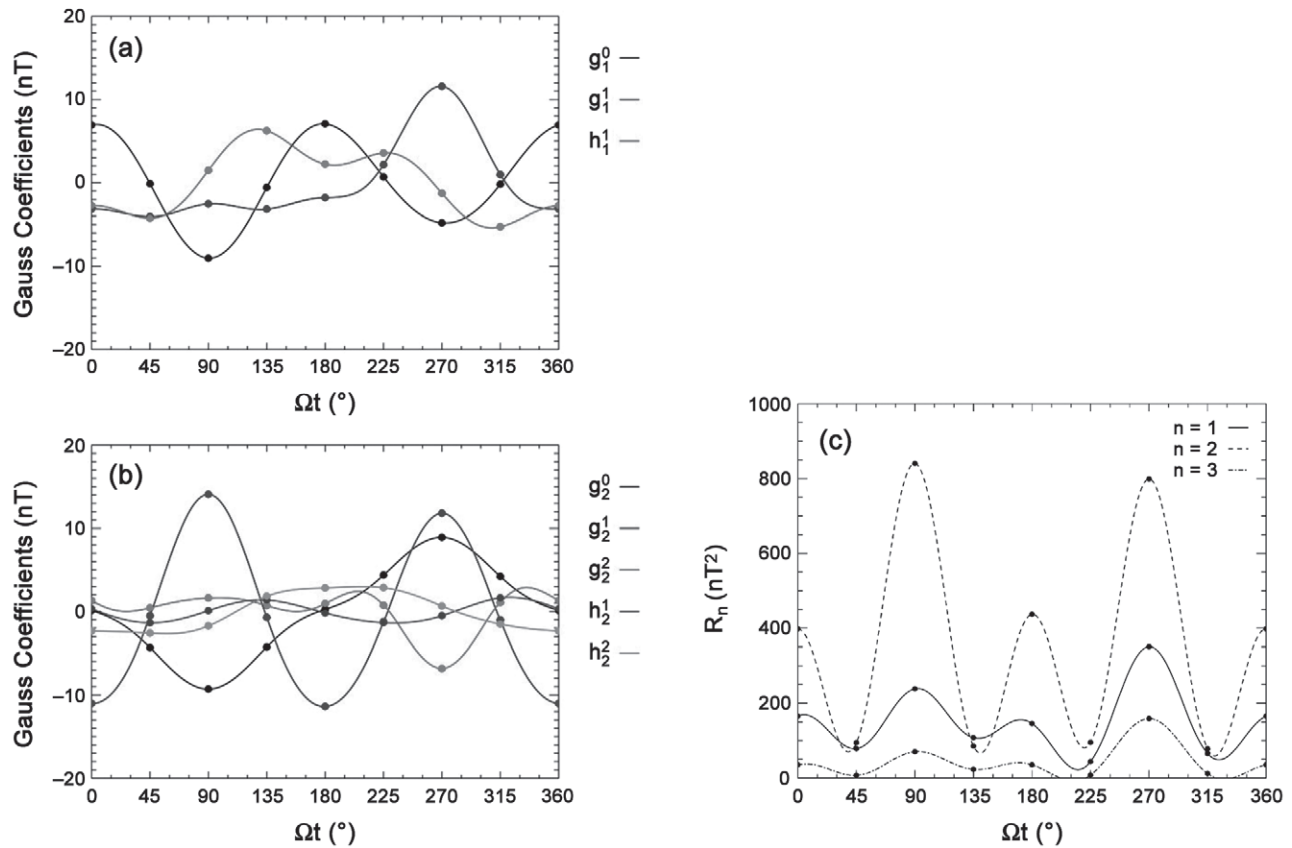


Fig. 10. See Plate 34. The spherical harmonic coefficients for the (a) dipolar and (b) quadrupolar terms induced by the Europa/plasma interaction over a synodic rotation period of Jupiter. (c) Total power contained in the induced field at the first three spherical harmonics. For comparison, the magnetic-field-induced dipole term contains power at the level of 14,000–88,000 nT^2 . Adapted from Schilling et al. (2007).

MgSO_4 concentration may be as little as $0.018 \text{ g MgSO}_4 \text{ kg}^{-1} \text{ H}_2\text{O}$. The models of Kargel et al. (2000) on the other hand yield extremely briny solutions with salt concentration as high as $560 \text{ g MgSO}_4 \text{ kg}^{-1} \text{ H}_2\text{O}$, whereas Zolotov and Shock's (2001) "total extraction" model can yield MgSO_4 concentration approaching $1000 \text{ g MgSO}_4 \text{ kg}^{-1} \text{ H}_2\text{O}$ (see Fig. 11). With such a divergent opinion on the concentration of the most noticeable salt on Europa's surface, it should be clear that there is currently no consensus on the concentrations of salts (or even their composition) in Europa's ocean. Further information on the current status of ocean composition can be found in the chapter by Zolotov and Kargel.

6.1. Relationship Between Salt Concentration and Conductivity

Hand and Chyba (2007) have recently combined the magnetometer-derived ocean conductivities with the interior models of Europa and the laboratory studies of conductivities of salt solutions to place better limits on the salinity of Europa's ocean. In order to obtain an empirical relationship between the salt concentration and the conductivity of the solution usable over a large range of salinity, Hand and Chyba (2007) compiled a dataset of experimental values of salt solution conductivities from a wide range

of sources and then scaled it to a common temperature of 0°C . Figure 12 reproduced from their work shows the conductivities of water solutions containing both sea salt (solid curve) and MgSO_4 (various symbols), which is the most likely salt in Europa's ocean. Also marked on the same figure are the upper and lower limits on the conductivities from the Zimmer et al. (2000) work. The lower limit from Zimmer et al. excludes the lowest partial extraction models of Zolotov and Shock (2001). The figure also shows that the conductivity of a MgSO_4 solution peaks at $\sim 6 \text{ S/m}$ at its dissolution saturation limit ($282 \text{ g kg}^{-1} \text{ H}_2\text{O}$), whereas for a NaCl solution the peak in conductivity occurs near 18 S/m , corresponding to a saturation limit of ($304 \text{ g kg}^{-1} \text{ H}_2\text{O}$).

6.2. Limits on the Salinity of the Ocean from Magnetic Field Observations

In order to further refine the limits on the salinity and thickness of Europa's ocean, Hand and Chyba (2007) used multiple-shell models of Europa's interior (ocean, mantle, and core) and its exterior (an ionosphere) to derive the response of Europa to the 11.1-h wave over a range of assumed ocean parameters such as the salinity, thickness, and depth from the surface. Figure 13 shows the relationship between ocean thickness and MgSO_4 concentration for an

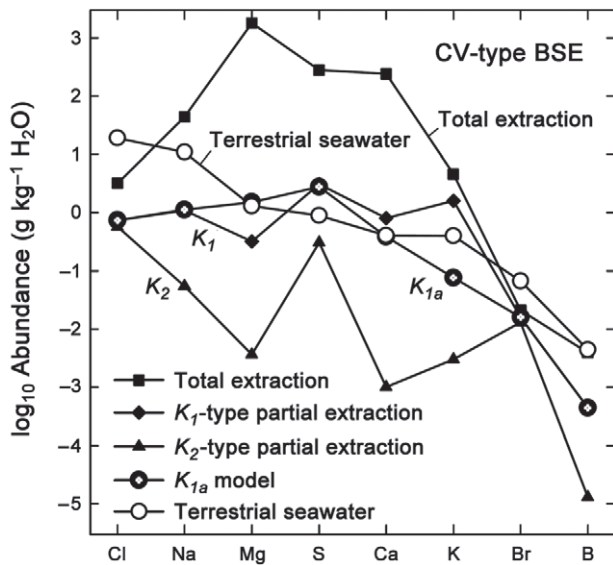


Fig. 11. Abundances of various elements for four different models of partial extraction from a 100-km-thick ocean in the models of *Zolotov and Shock* (2001). Their preferred model (K_{1a}) yields MgSO_4 concentration of $7.6 \text{ g MgSO}_4 \text{ kg}^{-1} \text{ H}_2\text{O}$. Adapted from *Zolotov and Shock* (2001).

assumed induction response factor of 0.7 [corresponding to the lower limit of *Zimmer et al.* (2000) estimates]. Calculations were performed for several different values of the icy shell thickness. As expected, there is an inverse rela-

tionship between the ocean thickness and the salinity of the ocean. The figure clearly illustrates the nonuniqueness problem arising from single-frequency measurements. The range of allowed parameters includes what would be considered fresh water by terrestrial standards with MgSO_4 concentrations below $1 \text{ g kg}^{-1} \text{ H}_2\text{O}$ to highly saline solutions containing salt concentrations as high as $16 \text{ g kg}^{-1} \text{ H}_2\text{O}$, corresponding to a 20-km-thick ocean buried under 60 km of ice.

Figure 14 from *Hand and Chyba* (2007) summarizes the response of Europa for a range of ocean conductivities, icy shell thicknesses, and ocean shell thicknesses calculated from the three-layer model introduced above. It can be seen that at the lower end of the response factor ($A \leq 0.75$), the ocean thickness and its conductivity can be traded to get the same response factor. However, as the amplitude of the response factor increases, the thickness of the ocean is not a strong factor in determining the response, but the ocean conductivity is. At the lower end of the response function estimates ($A = 0.75$) a freshwater ocean is clearly possible. However, if the response factor is 0.97 ± 0.02 as suggested by *Schilling et al.* (2004), only very thin ice shells (0–15 km) are allowed and the ocean would have to be hypersaline. *Hand and Chyba* (2007) also found that electromagnetic induction from an exterior ionosphere and/or a conducting inner layer (mantle or core) do not have an appreciable effect on the response from Europa at the 11.1-h wave period. On the other hand, the strong induction signature profoundly affects the strengths of the moon/plasma interaction currents and the magnetic field.

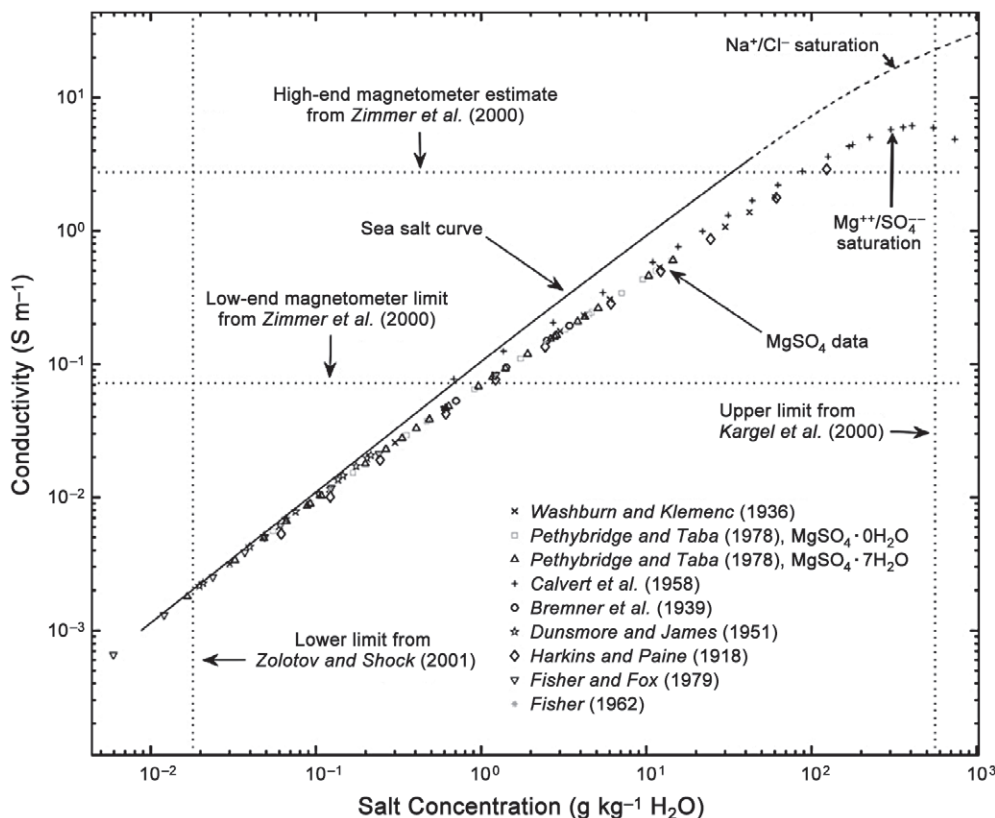


Fig. 12. Conductivities of water solutions containing sea salt (solid curve) and MgSO_4 (various symbols). The saturation points for NaCl ($304 \text{ g kg}^{-1} \text{ H}_2\text{O}$) and MgSO_4 ($282 \text{ g kg}^{-1} \text{ H}_2\text{O}$) are marked by short arrows. Adapted from *Hand and Chyba* (2007).

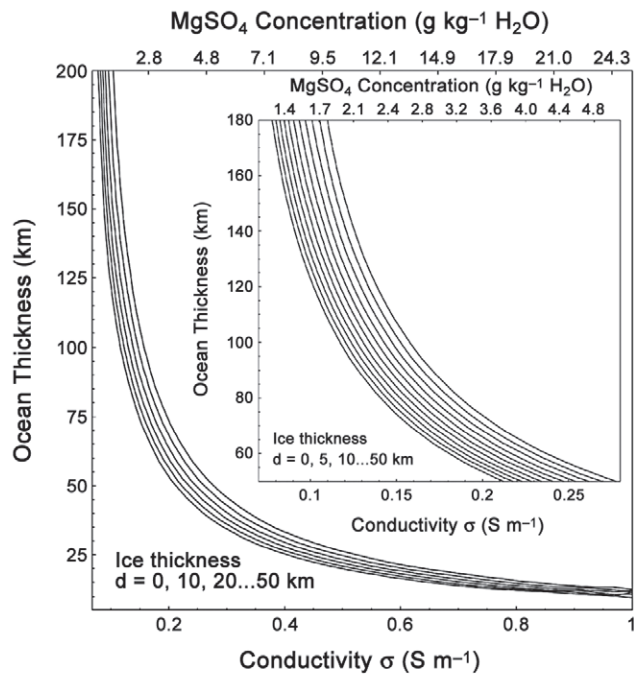


Fig. 13. The relationship between ocean thickness and MgSO_4 concentration for a given response factor of 0.7 corresponding to the lower limit of *Zimmer et al.* (2000) estimates. Curves were calculated for six different assumptions of ice shell thicknesses. Adapted from *Hand and Chyba* (2007).

7. SOUNDING THE DEEP INTERIOR OF EUROPA

So far we have focused exclusively on the induction response from the subsurface ocean at two principal frequencies associated with the rotation period of Jupiter and the orbital period of Europa. As the induction response of Europa's ocean at these frequencies is close to unity, most of the signal does not penetrate through the ocean. However, other frequencies must exist in the background magnetospheric field as Europa is located at the outer edge of Io's torus, an active region that responds continuously to changes in the density, magnetic flux, and energy content of the torus. It is believed that Io's torus responds to changes in the volcanic activity of Io over timescales of weeks to months. Thus Europa can be expected to be bathed in many different types of (although nonharmonic) frequencies. As already shown, longer-period waves penetrate a conductor more deeply, so we would like to assess the shielding efficiency of Europa's ocean to longer-period waves.

We have used the three-layer model of Europa's interior illustrated in Fig. 3 to calculate the response of Europa to waves of five different frequencies for a range of ocean thicknesses and an assumed conductivity of 2.75 S/m, similar to that of Earth's ocean (see Fig. 15). We find that for wave periods longer than three weeks, the shielding efficiency of Europa's ocean is less than 50%, suggesting that

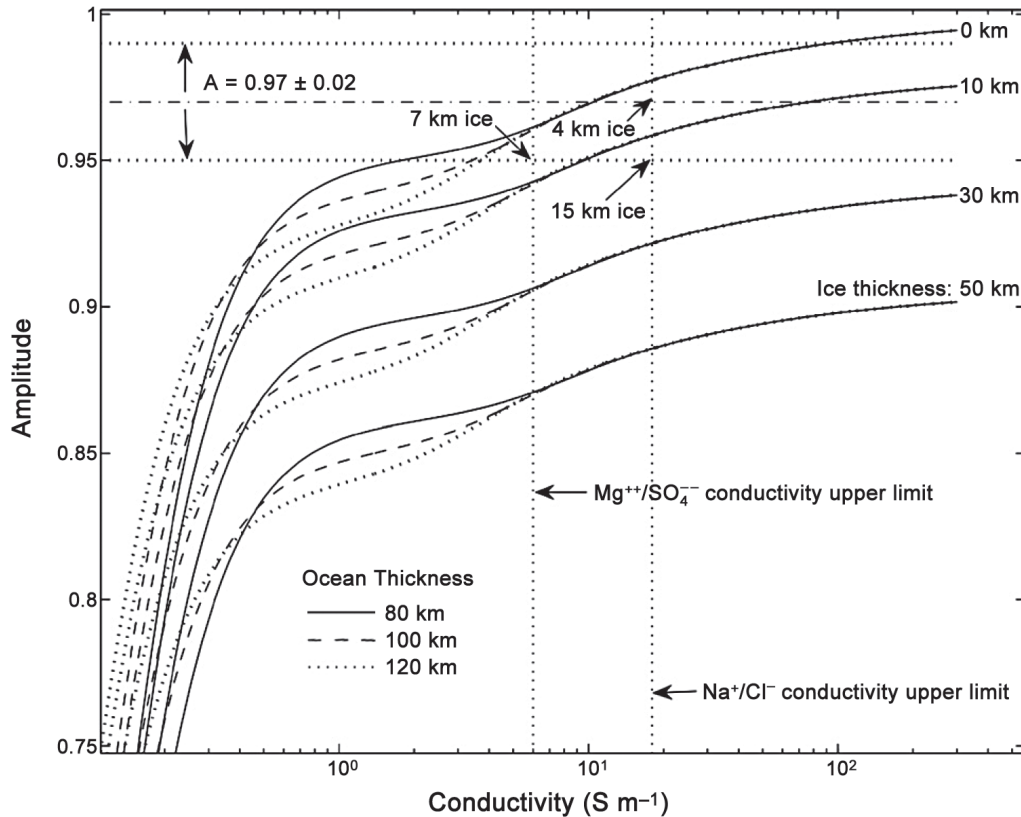


Fig. 14. The induction response factor as a function of conductivity, ocean thickness, and ice shell thickness for the three-layer model. Marked on the figure is the range of response factor deduced by *Schilling et al.* (2004) (horizontal dotted lines). The upper limit imposed on the conductivity of the solution from saturation effects are marked by the two vertical lines. Adapted from *Hand and Chyba* (2007).

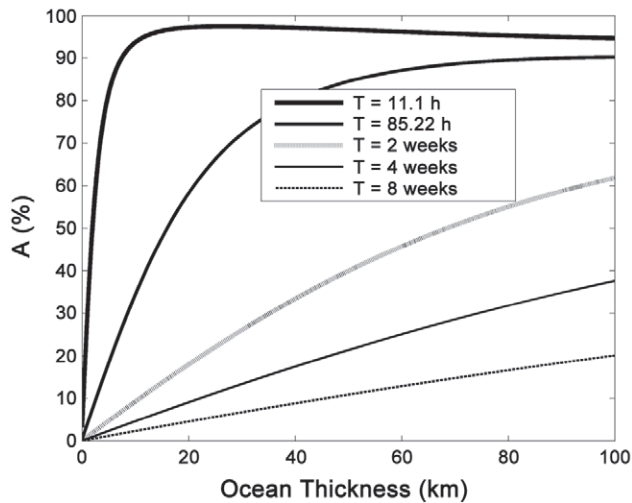


Fig. 15. Shielding efficiency of Europa's ocean to waves of five different periods for a range of ocean thicknesses. The assumed conductivity of the ocean is 2.75 S/m, similar to that of Earth's ocean.

roughly half of the signal is able to penetrate the ocean. Thus, if observations were available over periods of several months, it would become possible to assess Europa's response to deeper layers like the rocky mantle and especially the metallic core. As the conductivity of iron is many orders of magnitude higher than that expected of an ocean (see Table 1), the response factor of the core to wave periods of weeks to months would be close to 100% at its surface. If the core size is 50% of that of Europa (Anderson *et al.*, 1998), one can expect to see a response in the measured induction field at a level of ~6% of the original inducing signal, a small but certainly measurable signal.

8. FUTURE EXPLORATION USING ELECTROMAGNETIC INDUCTION

The exploration of Europa's interior using electromagnetic induction sounding is still in its infancy. The observations and associated modeling have been extremely basic because of the limited nature of observations that have been made so far during brief close flybys of Europa. Future continuous observations from one or more Europa orbiting spacecraft and multiple surface observatories could provide unprecedented capabilities allowing multiple-frequency sounding of Europa's ocean and its deeper interior.

In order to illustrate the power of long-period continuous data, we have computed several synthetic datasets mimicking observations from a Europa orbiter at an altitude of ~200 km. For these simulations we used the three-shell model of Fig. 3 and assumed that the conductivity of the ocean was 2.75 S/m, the inducing signal had a period of 11.1 h, and assigned a thickness to the exterior ice crust of 10 km. In Fig. 16, we plot the expected magnetic field data from three different assumptions about the ocean of Europa: no ocean (thin continuous line), a 3-km-thick ocean (dotted lines), and a deep ocean with a thickness of 100 km

(thick continuous lines). First of all, we would like to point out that from continuous time series, it is very easy to distinguish between the primary inducing field (external signal) at the synodic rotation period of Jupiter (large sinusoidal signal in all three components at a period of 11.1 h; thin continuous lines) and the dipolar induction response from the ocean (higher-frequency signal at the orbital frequency of the orbiter, internal signal). Thus, separating the signal into internal and external harmonics is quite straightforward. Next, as expected, we observe that a 100-km-thick ocean does induce a much stronger dipolar response (thick lines) than a 3-km-thick ocean (dotted lines), and data from an orbiter would be easily able to distinguish between the two scenarios. We have also experimented with including other wave periods such as the orbital period of Europa and find that it is possible to distinguish them from the 11.1-h period by Fourier transforming the continuous time series. Finally, we would like to point out that any departure of the ocean from a perfect spherical shape would lead to the generation of higher-degree (quadrupole and octupole) spherical harmonics in the data. Thus an examination of the induction field in terms of its harmonic content would yield information on the shape of the ocean.

Finally, we would like to point out that simultaneous measurements from multiple spacecraft or/and multiple surface sites facilitates the decomposition of the internal and external fields directly in time domain. The decomposed

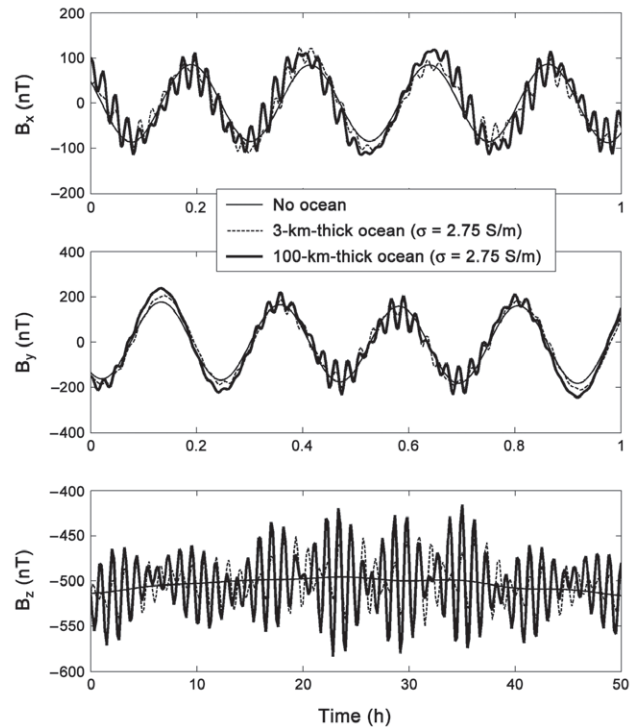


Fig. 16. Simulation of the expected magnetic field from a Europa orbiter orbiting at an altitude of ~200 km for three different assumptions about the ocean of Europa (no ocean, a 3-km-thick ocean, and a deep ocean with a thickness of 100 km). Further information on the properties of the ocean and the model is provided in the text of the chapter.

internal and external field time series can then be Fourier decomposed into the primary field and Europa's response at not only the two prime frequencies but also the weaker nonharmonic frequencies.

Acknowledgments. The authors would like to thank M. Volwerk and N. Schilling for several useful discussions. This work was supported by NASA grant NNX06AB91G. Portions of this work by K.P.H. were performed at the Jet Propulsion Laboratory, California Institute of Technology, under contract to the National Aeronautics and Space Administration.

REFERENCES

- Anderson J. D., Schubert G., Jacobson R. A., Lau E. L., Moore W. B., and Sjogren W. L. (1998) Europa's differentiated internal structure: Inferences from four Galileo encounters. *Science*, 281, 2019–2022.
- Bagenal F. and Sullivan J. D. (1981) Direct plasma measurements in the Io torus and inner magnetosphere of Jupiter. *J. Geophys. Res.*, 86, 8447–8466.
- Banks R. J. (1969) Geomagnetic variations and the conductivity of the upper mantle. *Geophys. J. R. Astron. Soc.*, 17, 457–487.
- Belcher J. W. (1983) The low energy plasma in the jovian magnetosphere. In *Physics of the Jovian Magnetosphere* (A. J. Dessler, ed.), pp. 68–105. Cambridge Univ., Cambridge.
- Carr M. H., Belton M. J. S., Chapman C. R., Davies M. E., Geissler P., Greenberg R., et al. (1998) Evidence for a subsurface ocean on Europa. *Nature*, 391, 363–365.
- Cassen P. M., Reynolds R. T., and Peale S. J. (1979) Is there liquid water on Europa? *Geophys. Res. Lett.*, 6, 731–734.
- Cassen P. M., Peale S. J., and Reynolds R. T. (1980) Tidal dissipation in Europa: A correction. *Geophys. Res. Lett.*, 7, 987–988.
- Chapman S. (1919) Solar and lunar diurnal variations of terrestrial magnetism. *Philos. Trans. Roy. Soc. Lond.*, A218, 1–118.
- Chapman S. and Price T. A. (1930) The electric and magnetic state of the interiors of the Earth, as inferred from terrestrial magnetic variations. *Philos. Trans. R. Soc. London*, A229, 427–460.
- Chapman S. and Whitehead T. T. (1922) Influence of electrically conducting material on phenomena of terrestrial magnetism. *Trans. Camb. Philos. Soc.*, 22, 463–482.
- Constable S. and Constable C. (2004) Observing geomagnetic induction in magnetic satellite measurements and associated implications for mantle conductivity. *Geochem. Geophys. Geosys.*, Q01006, DOI: 10.1029/2003GC000634.
- Didwall E. M. (1984) The electrical conductivity of the upper mantle as estimated from satellite magnetic field data. *J. Geophys. Res.*, 89, 537–542.
- Dyal P. and Parkin C. W. (1973) Global electromagnetic induction in the moon and planets. *Phys. Earth Planet. Inter.*, 7, 251–265.
- Fanale F. P., Li Y. H., De Carlo E., Farley C., Sharma S. K., and Horton K. (2001) An experimental estimate of Europa's "ocean" composition independent of Galileo orbital remote sensing. *J. Geophys. Res.*, 106, 14595–14600.
- Goertz C. K. (1980) Io's interaction with the plasma torus. *J. Geophys. Res.*, 85, 2949–2956.
- Greeley R., Sullivan R., Klemaszewski J., et al. (1998) Europa: Initial Galileo geological observations. *Icarus*, 135, 4–24.
- Hand K. P. and Chyba C. F. (2007) Empirical constraints on the salinity of the european ocean and implications for a thin ice shell. *Icarus*, 189, 424–438.
- Hobbs P. V. (1974) *Ice Physics*, pp. 97–120. Oxford Univ., London.
- Holzappel W. B. (1969) Effect of pressure and temperature on the conductivity and ionic dissociation of water up to 100 kbar and 1000°C. *J. Chemical Phys.*, 50, 4424–4428.
- Hood L. L., Mitchell D. L., Lin R. P., Acuna M. H., and Binder A. B. (1999) Initial measurements of the lunar induced dipole moment using Lunar Prospector magnetometer data. *Geophys. Res. Lett.*, 26, 2327–2330.
- Johnson F. S., ed. (1961) *Satellite Environment Handbook*. Stanford Univ., Stanford, California.
- Kargel J. S., Kaye J. Z., Head J. W. III, Marion G. M., Sassen R., Crowley J. K., Ballesteros O. P., Grand S. A., and Hogenboom D. L. (2000) Europa's crust and ocean: Origin, composition, and the prospects of life. *Icarus*, 148, 226–265.
- Khan A., Connolly J. A. D., Olsen N., and Mosegaard K. (2006) Constraining the composition and thermal state of the Moon from an inversion of electromagnetic lunar day-side transfer functions. *Earth Planet. Sci. Lett.*, 248, 579–598.
- Khurana K. K. (1997) Euler Potential models of Jupiter's magnetospheric field. *J. Geophys. Res.*, 102, 11295–11306.
- Khurana K. K. (2001) Influence of solar wind on Jupiter's magnetosphere deduced from currents in the equatorial plane. *J. Geophys. Res.*, 106, 25999–26016.
- Khurana K. K. and Kivelson M. G. (1989) Ultra low frequency MHD waves in Jupiter's middle magnetosphere. *J. Geophys. Res.*, 94, 5241.
- Khurana K. K., Kivelson M. G., Stevenson D. J., et al. (1998) Induced magnetic fields as evidence for subsurface oceans in Europa and Callisto. *Nature*, 395, 777–780.
- Khurana K. K., Kivelson M. G., and Russell C. T. (2002) Searching for liquid water on Europa by using surface observatories. *Astrobiology*, 2(1), 93–103.
- Kivelson M. G., Khurana K. K., Stevenson D. J., Bennett. L., Joy S., Russell C. T., Walker R. J., Zimmer C. and Polansky C. (1999) Europa and Callisto: Induced or intrinsic fields in a periodically varying plasma environment. *J. Geophys. Res.*, 104, 4609–4625.
- Kivelson M. G., Khurana K. K., Russell C. T., Volwerk M., Walker R. J., and Zimmer C. (2000) Galileo magnetometer measurements strengthen the case for a subsurface ocean at Europa. *Science*, 289, 1340.
- Kliore A. J., Hinson D. P., Flasar F. M., Nagy A. F., and Cravens T. E. (1997) The ionosphere of Europa from Galileo radio occultations. *Science*, 277, 355–358.
- Kliore A. J., Anabtawi A., and Nagy A. F. (2001) The ionospheres of Europa, Ganymede, and Callisto. *Eos Trans. AGU*, 82(47), Fall Meet. Suppl., Abstract B506.
- Lahiri B. N. and Price A. T. (1939) Electromagnetic induction in non-uniform conductors, and the determination of the conductivity of the earth from terrestrial magnetic variations. *Philos. Trans. R. Soc. London*, A237, 509–540.
- Lamb H. (1883) On electrical motions in a spherical conductor. *Philos. Trans. R. Soc. London*, 174, 519–549.
- Langel R. A. (1975) Internal and external storm-time magnetic fields from spacecraft data (abstract). In *IAGA Program Abstracts for XVI General Assembly*, Grenoble, France.
- Martinez Z. and McCreadie H. (2004) Electromagnetic induction modelling based on satellite magnetic vector data. *Geophys. J. Inter.*, 157, 1045–1060.
- McCord T. B., Hansen G. B., Fanale F. P., Carlson R. W., Matson D. L., et al. (1998) Salts on Europa's surface detected by Galileo's near infrared mapping spectrometer. *Science*, 280, 1242–1245.

- McCord T. B., Hansen G. B., Matson D. L., Johnson T. V., Crowley J. K., Fanale F. P., Carlson R. W., Smythe W. D., Martin P. D., Hibbitts C. A., Granahan J. C., and Ocampo A. (1999) Hydrated salt minerals on Europa's surface from the Galileo near-infrared mapping spectrometer (NIMS) investigation. *J. Geophys. Res.*, *104*, 11827–11851.
- McCord T. B., Orlando T. M., Teeter G., Hansen G. B., Sieger M. T., Petrik N. G., and Keulen L. V. (2001) Thermal and radiation stability of the hydrated salt minerals epsomite, mirabilite, and natron under Europa environmental conditions. *J. Geophys. Res.*, *106*, 3311–3319.
- McCord T. B., Teeter G., Hansen G. B., Sieger M. T., and Orlando T. M. (2002) Brines exposed to Europa surface conditions. *J. Geophys. Res.*, *107*(E1), 4.1–4.6, DOI: 10.1029/2000JE001453.
- McKinnon W. B. and Zolensky M. E. (2003) Sulfate content of Europa's ocean and shell: Evolutionary considerations and some geological and astrobiological implications. *Astrobiology*, *3*, 879–897.
- Montgomery R. B. (1963) Oceanographic data. In *American Institute of Physics Handbook* (D. E. Gray, ed.), pp. 125–127. McGraw-Hill, New York.
- Neubauer F. M. (1980) Nonlinear standing Alfvén wave current system at Io: Theory. *J. Geophys. Res.*, *85*, 1171–1178.
- Neubauer F. M. (1998) The sub-Alfvénic interaction of the Galilean satellites with the jovian magnetosphere. *J. Geophys. Res.*, *103*, 19834–19866.
- Neubauer F. M. (1999) Alfvén wings and electromagnetic induction in the interiors: Europa and Callisto. *J. Geophys. Res.*, *104*, 28671–28684.
- Olhoef G. R. (1989) Electrical properties of rocks. In *Physical Properties of Rocks and Minerals* (Y. S. Touloukian et al., eds.), pp. 257–329. Hemisphere Publishing, New York.
- Olsen N. (1999a) Long-period (30 days–1 year) electromagnetic sounding and the electrical conductivity of the lower mantle beneath Europe. *Geophys. J. Inter.*, *138*, 179–187.
- Olsen N. (1999b) Induction studies with satellite data. *Surv. Geophys.*, *20*, 309–340.
- Pappalardo R. T., Head J. W., Greeley R., et al. (1998) Geological evidence for solid-state convection in Europa's ice shell. *Nature*, *391*, 365–368.
- Pappalardo R. T., Belton M. J. S., Breneman H. H., et al. (1999) Does Europa have a subsurface ocean? Evaluation of the geological evidence. *J. Geophys. Res.*, *104*, 24015–24055.
- Parkinson W. D. (1983) *Introduction to Geomagnetism*. Scottish Academic, Edinburgh.
- Russell C. T., Coleman P. J. Jr., and Goldstein B. E. (1981) Measurements of the lunar induced magnetic moment in the geomagnetic tail: Evidence for a lunar core? *Proc. Lunar Planet. Sci. Conf. 12th*, pp. 831–836.
- Saur J., Strobel D. F., and Neubauer F. M. (1998) Interaction of the jovian magnetosphere with Europa: Constraints on the neutral atmosphere. *J. Geophys. Res.*, *103*, 19947–19962.
- Schilling N., Khurana K. K., and Kivelson M. G. (2004) Limits on an intrinsic dipole moment in Europa. *J. Geophys. Res.*, *109*, E05006, DOI: 10.1029/2003JE002166.
- Schilling N., Neubauer F. M., and Saur J. (2007) Time-varying interaction of Europa with the jovian magnetosphere: Constraints on the conductivity of Europa's subsurface ocean. *Icarus*, *192*, 41–55, DOI: 10.1016/j.icarus.2007.06.024.
- Schilling N., Neubauer F. M., and Saur J. (2008) Influence of the internally induced magnetic field on the plasma interaction of Europa. *J. Geophys. Res.*, *113*, A03203, DOI: 10.1029/2007JA012842.
- Schultz A. and Larsen J. C. (1987) On the electrical conductivity of the mid-mantle: 1. Calculation of equivalent scalar magnetotelluric response functions. *Geophys. J. R. Astron. Soc.*, *88*, 733–761.
- Schubert G., Lichtenstein B. R., Coleman P. J., and Russell C. T. (1974) *J. Geophys. Res.*, *79*, 2007–2013.
- Schuster A. (1886) On the diurnal period of terrestrial magnetism. *Philos. Mag.*, *5*, Series 21, S.349–S.359.
- Schuster A. (1889) The diurnal variation of terrestrial magnetism. *Philos. Trans. R. Soc.*, A 180, 467–518.
- Shoemaker E. M. and Wolfe R. F. (1982) Cratering time scales for the Galilean satellites. In *Satellites of Jupiter* (D. Morrison, ed.), pp. 277–339. Univ. of Arizona, Tucson.
- Sonett C. P. (1982) Electromagnetic induction in the Moon. *Rev. Geophys. Space Phys.*, *20*, 411.
- Velimsky J., Martinec Z., and Everett M. E. (2006) Electrical conductivity in the Earth's mantle inferred from CHAMP satellite measurements — 1. Data processing and 1-D inversion. *Geophys. J. Inter.*, *166*, 529–542.
- Volwerk M., Kivelson M. G., and Khurana K. K. (2001) Wave activity in Europa's wake: Implications for ion pickup. *J. Geophys. Res.*, *106*, 26033–26048.
- Volwerk M., Khurana K., and Kivelson M. (2007) Europa's Alfvén wings: Shrinkage and displacement influenced by an induced magnetic field. *Ann. Geophys.*, *25*, 905–914.
- Zahnle K., Dones L., and Levison H. F. (1998) Cratering rates on the Galilean satellites. *Icarus*, *136*, 202–222.
- Zimmer C., Khurana K. K., and Kivelson M. G. (2000) Subsurface oceans on Europa and Callisto: Constraints from Galileo magnetometer observations. *Icarus*, *147*, 329–347.
- Zolotov M. Y. and Shock E. L. (2001) Composition and stability of salts on the surface of Europa and their oceanic origin. *J. Geophys. Res.*, *106*, 32815–32827.